

**SUPPLEMENTARY INFORMATION for:**

**ALL-SILICONE ELASTIC COMPOSITES WITH COUNTER-INTUITIVE  
PIEZOELECTRIC RESPONSE, DESIGNED FOR ELECTROMECHANICAL  
APPLICATIONS**

**Carmen Racles<sup>a\*</sup>, Mihaela Dascalu<sup>a</sup>, Adrian Bele<sup>a</sup>, Vasile Tiron<sup>b</sup>, Mihai  
Asandulesa<sup>a</sup>, Codrin Tugui<sup>a</sup>, Ana-Lavinia Vasiliu<sup>a</sup>, Maria Cazacu<sup>a</sup>**

*<sup>a</sup> "Petru Poni" Institute of Macromolecular Chemistry, Aleea Grigore Ghica Voda, 41A, 700487 Iasi, Romania*

*<sup>b</sup> Research Department, Faculty of Physics, Alexandru Ioan Cuza University of Iasi, Blvd. Carol I No. 11, 700506 Iasi, Romania*

*\* e-mail: raclesc@icmpp.ro*



**Figure S1:** Cl-modified silicone mixed with PDMS and cross-linked together (left) versus PDMS –polar particles composite film (right)

**Infrared spectroscopy**

The cyclic nature of CMV compound was supported by the absence of Si-OH band at 3690  $\text{cm}^{-1}$  in the FT-IR spectrum as well as by the shape of the siloxane band (Figure S2). It is well-established that cyclic trimers have an absorption band at 1010-1020  $\text{cm}^{-1}$ , cyclic tetramers and pentamers at 1070-1090  $\text{cm}^{-1}$ , while for larger compounds the Si-O-Si band widens and splits.<sup>S1</sup> In our case, the shape and position of the Si-O-Si band, at 1076  $\text{cm}^{-1}$  point towards a tetramer majority species, which is in agreement with H NMR (Figure S3). The Si(CH<sub>3</sub>) bands are at 1261, 808 and 852  $\text{cm}^{-1}$ , while the Si-CH=CH<sub>2</sub> specific bands were found at: 961 and 1011  $\text{cm}^{-1}$ , 1408 and 1599  $\text{cm}^{-1}$ . After photo-addition, the bands

corresponding to the vinyl group disappeared and weak bands are observed at 1420 and 2852  $\text{cm}^{-1}$  that could be assigned to (S-)CH<sub>2</sub> bonds (stretch asymmetric and  $\delta$ , respectively).<sup>S2</sup>

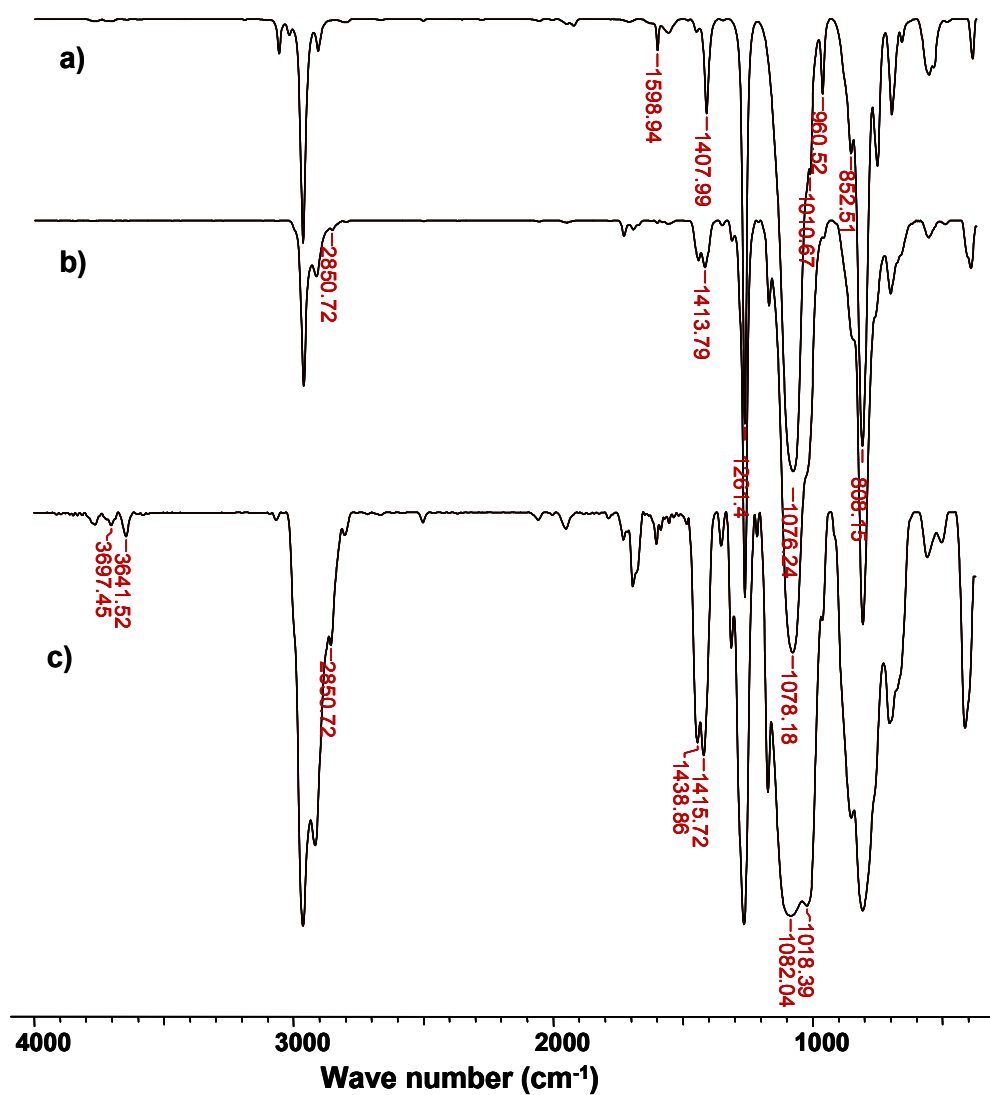


**Figure S2:** FT-IR spectra of CMV (a), Cl-23 (b) and Cl-33P (c)

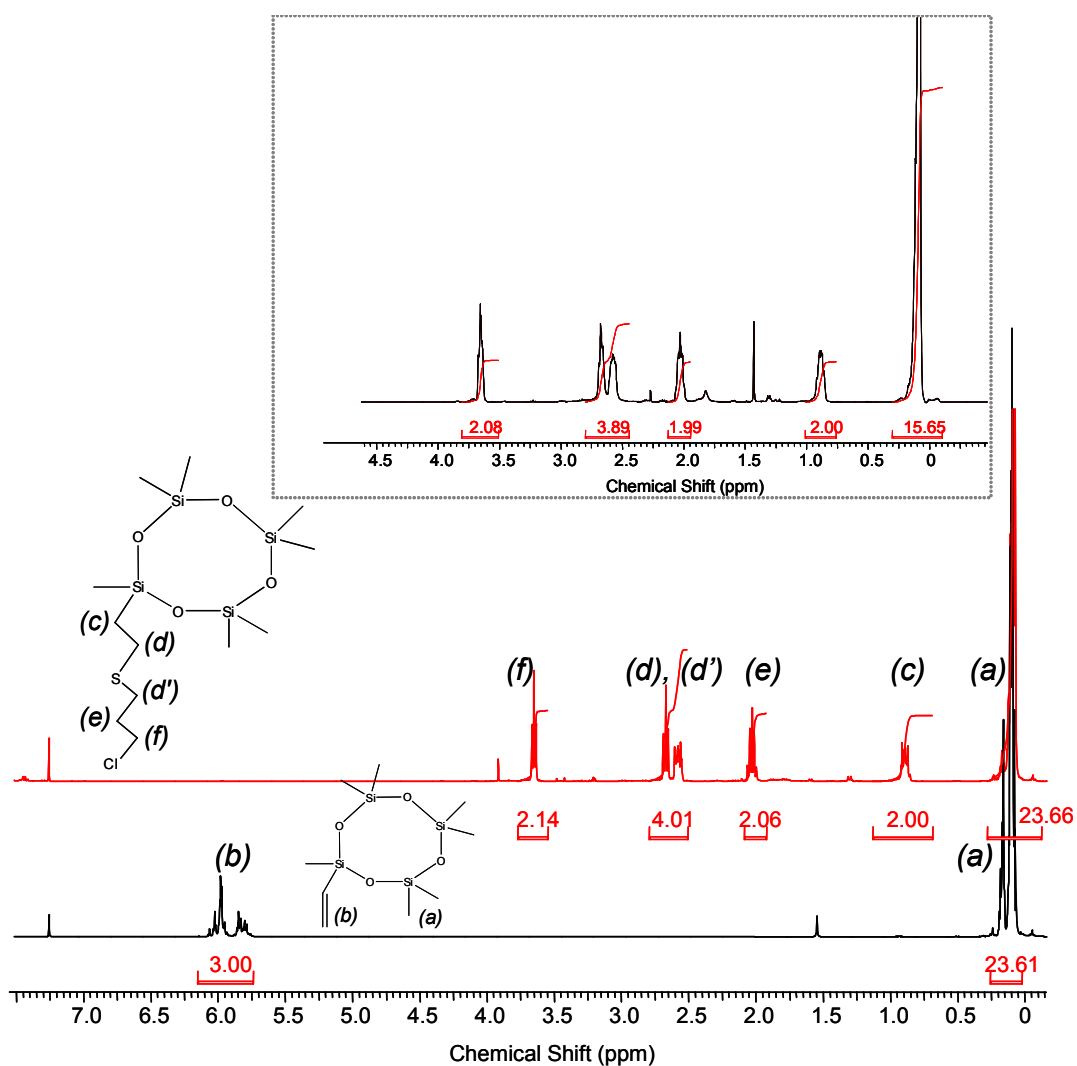


**Figure S3:**  $^1\text{H}$  NMR spectrum of methyl-vinyl cyclosiloxane (bottom), Cl-23 (up) and the corresponding copolymer Cl-33P (inset)

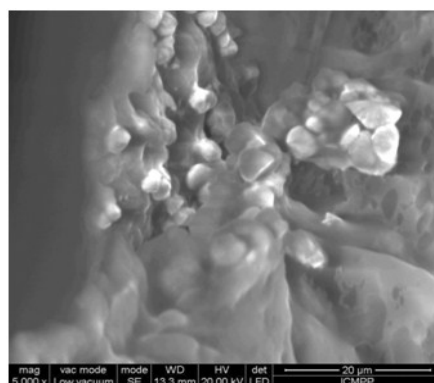


**Figure S4:** SEM image of a composite having PDMS matrix and a siloxane copolymer with 62 mol% CN groups as particles stabilized with a siloxane surfactant

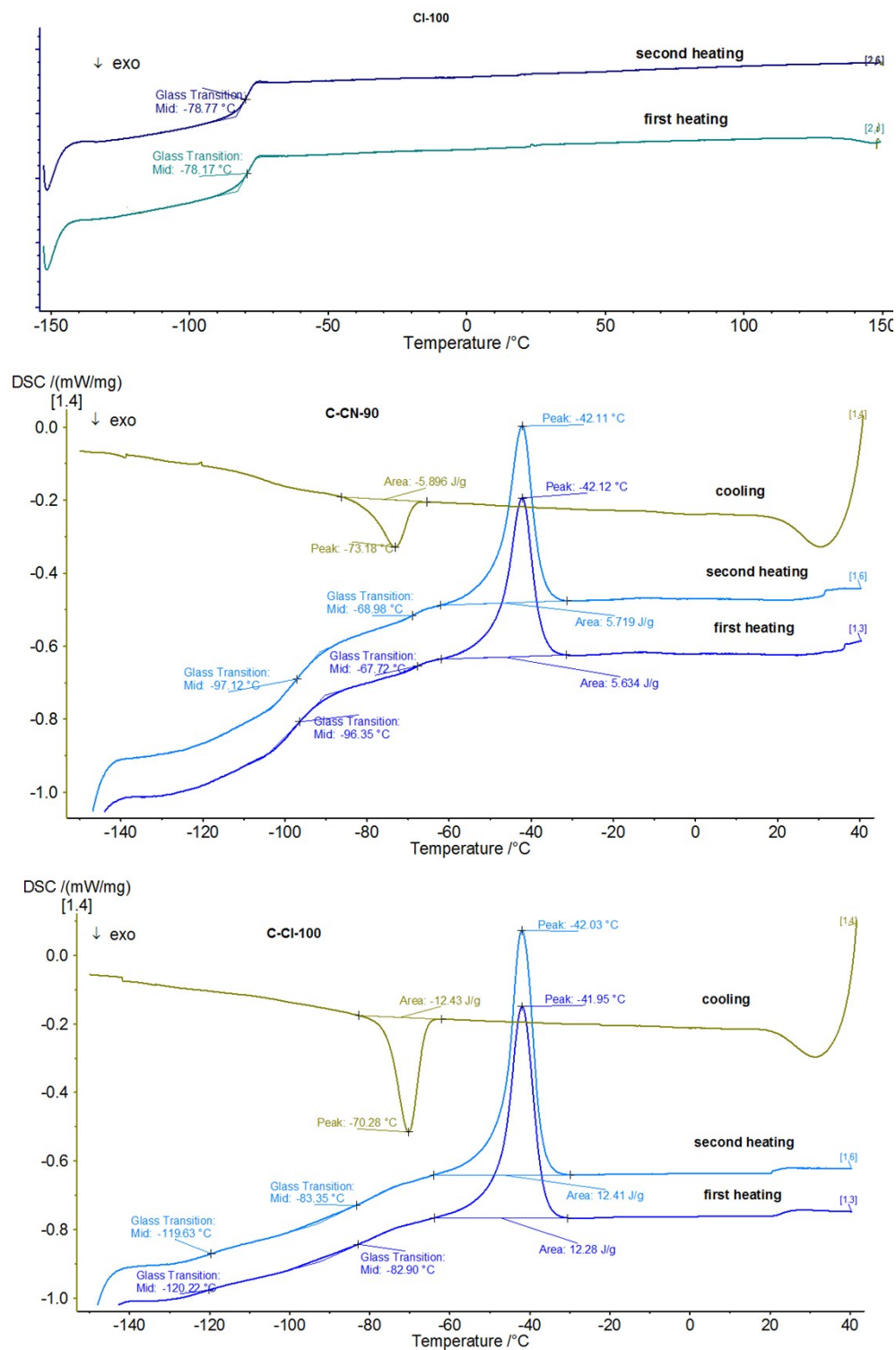


**Figure S5:** DSC curves of CI-100 and composites C-CN-90 and C-CI-100

**Table S1:** Calculated solubility parameters and density<sup>S3</sup> of the components of all-silicone composites

Code	CI-23	CI-100	CN-25	CN-90	Pluronic L81	PDMS
$\delta$ , (cal·cm <sup>-3</sup> ) <sup>0.5</sup>	8.05	9.24	8.01	9.46	10.21	7.4
$d$ , g·cm <sup>-3</sup>	1.0086	1.1144	0.9515	1.0335	1.1048	0.97*

\* According to ref.<sup>S4</sup>

**The complex dielectric permittivity** at room temperature was recorded by sweeping frequency from 0.1 to 10<sup>6</sup> Hz, using a Novocontrol Dielectric Spectrometer equipped with frequency response analyzer. For measuring liquid samples the polymer was pressed between two electrodes ( $\varnothing = 20$  mm) while the samples thickness was adjusted with glass spacers to 140  $\mu$ m and the material in excess was removed. The free-standing films were sandwiched between two gold-plated electrodes ( $\varnothing = 20$  mm) and the analyses have been carried out in dry nitrogen atmosphere. For variable temperature measurements, the Quatro Cryosystem has been used in order to set the temperature of the analyzed sample with 0.1°C stability within the range of -150°C – 40°C.

The **effective dielectric constant** of a heterogeneous dielectric with two phases is estimated as:

$$\varepsilon_{eff}^n = v_1 \varepsilon_1^n + v_2 \varepsilon_2^n \quad (1)$$

where  $\varepsilon_1$  and  $\varepsilon_2$  are the dielectric permittivity of the phases (matrix and filler, respectively),  $v_1$  and  $v_2$  are the volume fractions,  $n$  is the structural index of the mixture ( $-1 \leq n \leq 1$ ).<sup>S5,S6</sup> The lower and upper limits of dielectric permittivity of the composite may be expressed as:

$$\varepsilon_{min} = v_1 \varepsilon_1 + v_2 \varepsilon_2 \quad (2)$$

$$\varepsilon_{max} = \varepsilon_1 \varepsilon_2 / (v_2 \varepsilon_1 + v_1 \varepsilon_2) \quad (3)$$

The volume fractions were calculated using density data from Table S1.

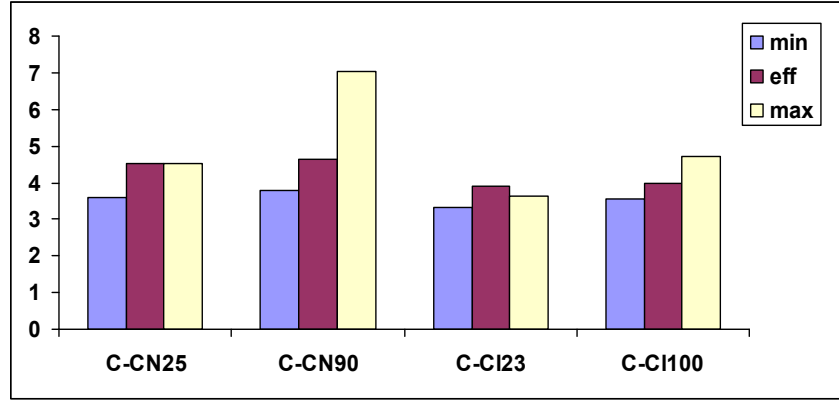


**Figure S6:** Dielectric constant of the composites measured at 10 kHz ( $\epsilon_{\text{eff}}$ ) and its limits calculated with the mixing rule

**The Havriliak- Negami equation:**<sup>S7</sup>

$$\epsilon^* = \epsilon' - i\epsilon'' = \epsilon_{\infty} + \frac{\epsilon_s - \epsilon_{\infty}}{[1 + (i\omega\tau_{HN})^a]^b} \quad (4)$$

where  $\Delta\epsilon = \epsilon_s - \epsilon_{\infty}$  represents the intensity of relaxation, i.e., the difference between the real permittivity values at the low ( $\omega \rightarrow 0$ ) and respectively, high ( $\omega \rightarrow \infty$ ) frequency limits,  $\omega = 2\pi f$  represents the angular frequency,  $f$  is the frequency,  $\tau$  is the relaxation time for each process associated with peak maxima, and  $a$  and  $b$  represent the broadening and skewing parameters, respectively. WinFIT software provided with Novocontrol dielectric spectrometer was used for data fit.

**Piezoelectric force microscopy (PFM)** technique was employed for quantitative determination of the longitudinal piezoelectric coefficient  $d_{33}$  using a multimode AFM microscope (NT-MDT SolvePro) equipped with a PFM measurement option. Microscope controlling, acquisition and analysis of the data were done by using *Nova* software. **PFM** technique is able to use inverse piezoelectric effect to obtain local polarization of electric dipoles. PFM technique is based on the detection of the local electromechanical vibration of the sample caused by an external alternating voltage applied between the conductive AFM-tip and the investigated sample. The external electric field causes a piezoelectric deformation of the material underneath the tip, both out-of-plane and in-plane. The out-of-plane deformation is measured by the deflection of the cantilever, while in-plane deformation is measured by torsion of the cantilever. In this experiment, only out-of-plane deformation was measured, which allows to determine only the longitudinal piezoelectric coefficient  $d_{33}$ . All PFM images were taken during one imaging session with the same cantilever (nominal spring constant 2.8

N·m<sup>-1</sup> and free resonant frequency of 197.2 kHz) and laser position in order to allow for quantitative comparison across the samples investigated. PFM measurements (surface topography, phase and amplitude of piezoresponse) over surface area 20×20 μm<sup>2</sup>, were performed in contact mode, in air, at room temperature, using vertical set-point deflection of 2 nm, amplitude AC voltage of 1 V and scanning speed of 0.8 Hz. The average value of the longitudinal piezoelectric constant ( $d_{33}$ ) was evaluated by recording piezoresponse curves in 100 equidistant points placed over five random surfaces with size area of 20×20 μm<sup>2</sup>. The piezoresponse curves were obtained by sweeping DC bias voltage and the piezoelectric constant was calculated from the slope of the linear dependence of piezoresponse amplitude on bias voltage.

## References

- S1. P. J. Launer, in *Silicone Compounds Register and Review*, ed. B. Arkles, Petrarch Systems, 1987.
- S2. E. Pretsch, P. Bühlmann and M. Badertscher, *Structure Determination of Organic Compounds, Tables of Spectral Data*, Fourth, Revised and Enlarged Edition Springer-Verlag Berlin Heidelberg 2009.
- S3. J. Bicerano, *Prediction of Polymer Properties*, Third Edition, Revised and Expanded, Marcel Dekker Inc. New York Basel, 2002.
- S4. A. C. M. Kuo, in *Polymer Data Handbook*, 1999, Oxford University Press, 411-435.
- S5. F. B. Madsen, A. E. Daugaard, S. Hvilsted and A. L. Skov, *Macromol. Rapid Commun.*, 2016, **37**, 378–413.
- S6. C. Zhang, D. Wang, J. He, M. Liu, G. H. Hu and Z. M. Dang, *Polym. Chem.*, 2014, **5**, 2513-2520.
- S7. S. Havriliak and S. Negami, *Polymer* 1967, **8**, 161–210.